

# Description of the candidate chiral doublet bands in $^{98}\text{Tc}^*$

QI Bin(齐斌)<sup>1)</sup> ZHANG Pan(张盼) ZHANG Jing(张靖) FU Jie(付捷)  
LI Yu-Qi(李昱琪) SONG He-He(宋鹤鹤) WANG Shou-Yu(王守宇)

School of Space Science and Physics, Shandong University at Weihai, Weihai 264209, China

**Abstract:** The candidate chiral doublet bands in  $^{98}\text{Tc}$  with configuration  $\pi g_{9/2} \otimes \nu h_{11/2}$  are studied theoretically for the first time via the triaxial particle rotor model. The main properties of the doublet bands including the energy spectra and electromagnetic transitions are calculated for different triaxiality parameter  $\gamma$ , and the data in  $^{98}\text{Tc}$  can be well described by the calculations with  $\gamma = 38^\circ$ . Based on the analysis of angular momentum components, it is found that the chiral rotational geometry in  $^{98}\text{Tc}$  deviates from the ideal chiral picture.

**Key words:** chiral doublet bands,  $^{98}\text{Tc}$ , particle rotor model

**PACS:** 21.60.Ev, 21.10.Re, 23.20.Lv **DOI:** 10.1088/1674-1137/36/10/007

## 1 Introduction

Since the theoretical prediction of spontaneous chiral symmetry breaking in nuclear structures in 1997 [1], many efforts have been made to further explore this interesting phenomenon. So far, about 30 candidate chiral nuclei have been reported experimentally in the  $A \approx 80, 100, 130$  and 190 mass regions. An overview of these studies and open problems in understanding the nuclear chirality is introduced in Ref. [2].

In the  $A \approx 100$  mass region, the candidate chiral doublet bands have been reported in  $^{102,103,104,105,106}\text{Rh}$  [3–5] and  $^{105,106}\text{Ag}$  [6, 7]. The corresponding configurations were suggested as  $\pi g_{9/2}^{-1} \otimes \nu h_{11/2}$  for odd-odd nuclei and  $\pi g_{9/2}^{-1} \otimes (\nu h_{11/2})^2$  for odd- $A$  nuclei. For the odd-odd Ag and Rh isotopes, the neutron Fermi levels are supposed to lie in the bottom of  $\nu h_{11/2}$  subshell and the proton Fermi levels are supposed to lie in the upper  $\pi g_{9/2}$  subshell. Recently, the candidate chiral doublet bands with configuration  $\pi g_{9/2} \otimes \nu h_{11/2}$  have been also reported in Tc isotopes, namely  $^{100}\text{Tc}$  [8] and  $^{98}\text{Tc}$  [9]. Compared with Ag ( $Z = 45$ ) and Rh ( $Z = 47$ ) isotopes, the pro-

ton Fermi levels in Tc isotopes ( $Z = 43$ ) are more likely to be close in the middle of the  $\pi g_{9/2}$  subshell. Therefore it is interesting to examine the candidate chiral bands in Tc isotopes, in which the configuration deviates from the ideal particle-hole configuration.

On the theoretical side, describing quantitatively the candidate chiral doublet bands can be carried out by either the triaxial particle rotor model (PRM) [10, 11] or random phase approximation calculations based on the tilted axis cranking model [12]. Using PRM, which couples two quasiparticles to a rigid triaxial rotor [10], the candidate chiral doublet bands in  $^{106}\text{Rh}$  [13, 14] and  $^{100}\text{Tc}$  [8] have been studied. Using PRM, which couples many particles to a rigid triaxial rotor [11], the candidate chiral doublet bands in the odd- $A$  nuclei  $^{103,105}\text{Rh}$  have been described very well [15, 16]. However, for  $^{98}\text{Tc}$  [9], such quantitative comparison between the expectations for the chiral scenario and the observation is still scarce.

Based on the above considerations, in this paper, the candidate chiral doublet bands in  $^{98}\text{Tc}$  will be studied via the triaxial PRM. The energy spectra and the electromagnetic transition ratios of the doublet bands in  $^{98}\text{Tc}$  will be calculated and compared with

Received 20 February 2012

\* Supported by National Natural Science Foundation of China (11005069, 11175108) and Shandong Natural Science Foundation (ZR2010AQ005)

1) E-mail: bqi@sdu.edu.cn

©2012 Chinese Physical Society and the Institute of High Energy Physics of the Chinese Academy of Sciences and the Institute of Modern Physics of the Chinese Academy of Sciences and IOP Publishing Ltd

the available data. Their chiral geometry will be discussed. Meanwhile, the influence of the triaxial deformation  $\gamma$  on the properties of the doublet bands with configuration  $\pi g_{9/2} \otimes \nu h_{11/2}$  will also be investigated.

## 2 Model

The particle rotor model has been extensively used in the investigation of the chiral rotation. The detailed formulae for the adopted PRM which couples two quasiparticles to a rigid triaxial rotor are described in Ref. [10]. Here just a brief introduction for this model is given.

The PRM Hamiltonian with one particle and one hole coupled with a triaxial rotor, which is used to describe the ideal chiral doublet bands, can be written as [1, 17, 18]

$$\hat{H} = \hat{H}_{\text{core}} + \hat{H}_{\text{p}} + \hat{H}_{\text{n}}, \quad (1)$$

where  $\hat{H}_{\text{core}}$  represents the Hamiltonian of the rotor

$$\hat{H}_{\text{core}} = \sum_{\nu=1}^3 \frac{(I_{\nu} - j_{\text{p}\nu} - j_{\text{n}\nu})^2}{2\mathcal{J}_{\nu}}, \quad (2)$$

$\mathcal{J}_{\nu} (\nu = 1, 2, 3)$  is the irrotational moment of inertia  $\mathcal{J}_{\nu} = \mathcal{J} \sin^2 \left( \gamma - \frac{2\pi}{3} \nu \right)$  ( $\nu = 1, 2, 3$ ),  $H_{\text{p}}$  and  $H_{\text{n}}$  describe the Hamiltonians of the single proton and neutron outside the rotor which for a single- $j$  model can be given as

$$H_{\text{p(n)}} = \pm \frac{1}{2} C \left\{ \cos \gamma \left( j_3^2 - \frac{j(j+1)}{3} \right) + \frac{\sin \gamma}{2\sqrt{3}} (j_+^2 + j_-^2) \right\}, \quad (3)$$

where the plus sign refers to a particle and the minus to a hole and the coupling parameter  $C$  is proportional to the quadrupole deformation  $\beta$ .

Including the pairing by the standard BCS quasiparticle approximation, the PRM can be generalized to the two quasiparticles coupled with a triaxial rotor cases. In this model, the single-particle energy  $\epsilon_{\nu}$  obtained by diagonalizing the single proton (neutron) Hamiltonian is replaced with the corresponding quasiparticle energy  $E_{\nu}$ ,

$$E_{\nu i} = \sqrt{(\epsilon_{\nu i} - \lambda_i)^2 + \Delta_i^2}, \quad i = \text{n, p}, \quad (4)$$

where  $\epsilon_{\nu i}$  is the single particle energy,  $\Delta_i$  the pairing gap and  $\lambda_i$  the Fermi energy. In comparison with the case excluding pairing, each single-particle matrix element needs to be multiplied by a pairing factor  $u_{\mu} u_{\nu} + v_{\mu} v_{\nu}$  [10], in which the pairing occupation

factor  $v_{\nu}$  of the state  $\nu$  is given by

$$v_{\nu}^2 = \frac{1}{2} \left[ 1 - \frac{\epsilon_{\nu} - \lambda}{E_{\nu}} \right], \quad (5)$$

and  $u_{\nu}^2 + v_{\nu}^2 = 1$ .

## 3 Results

### 3.1 Parameters

For nucleus  $^{98}\text{Tc}$ , the total Routhian surface (TRS) calculations have been carried out in Ref. [9], and the obtained deformation parameters ( $\beta$ ,  $\gamma$ ) change from  $(0.158, -6^{\circ})$  at the rotational frequency  $\hbar\omega = 0$  to  $(0.182, -37^{\circ})$  at  $\hbar\omega = 0.5$  MeV. In addition, it has been found [10, 18] that the properties of chiral doublet bands are very sensitive to the parameter  $\gamma$  but not so sensitive to  $\beta$ . Thus, in the present calculations, the quadrupole deformation  $\beta$  is fixed as 0.182, and the triaxiality parameter  $\gamma$  take the values from  $14^{\circ}$  to  $46^{\circ}$ . The configuration  $\pi g_{9/2} \otimes \nu h_{11/2}$  is adopted according to the configuration assignment in Ref. [9]. The pairing gap  $\Delta = 12/\sqrt{A} \approx 1.2$  MeV is used. The neutron Fermi energy is supposed to lie in the bottom of  $\nu h_{11/2}$  subshell. The proton Fermi energies take the values of  $(\epsilon_3 + \epsilon_4)/2$ , where  $\epsilon_i$  ( $i=1, 2, 3, 4, 5$ ) are obtained by diagonalizing the single proton Hamiltonian of Eq. (3) in the  $\pi g_{9/2}$  subshell. The moment of inertia takes the value of  $20 \hbar^2 \text{MeV}^{-1}$  according to the slope of the experimental energies versus  $I$  curve. For the electromagnetic transition, the empirical intrinsic quadrupole moment  $Q_0 = 4$  eb, gyromagnetic ratios  $g_{\text{R}} = Z/A = 0.44$ ,  $g_{\text{p}}(\pi g_{9/2}) = 1.26$ , and  $g_{\text{n}}(\nu h_{11/2}) = -0.21$  are adopted.

### 3.2 Energy spectra

The energy spectra of the two lowest bands A and B in  $^{98}\text{Tc}$  calculated by PRM with the configuration  $\pi g_{9/2} \otimes \nu h_{11/2}$  for different triaxiality parameter  $\gamma$  are shown in Fig. 1. It can be found that the energy differences between the two bands are smaller for small  $\gamma$  values, while relatively larger for  $\gamma > 34^{\circ}$  (larger than 400 keV). The smallest energy difference between the doublet bands occurs at spin  $I = 14 \hbar$  for  $\gamma = 14^{\circ}, 18^{\circ}, 22^{\circ}$ , at spin  $I = 12 \hbar$  for  $\gamma = 26^{\circ}, 30^{\circ}, 34^{\circ}, 38^{\circ}$  and at spin  $I = 10 \hbar$  for  $\gamma = 42^{\circ}, 46^{\circ}$ . These properties are very different from the results of the symmetric particle-hole configuration  $\pi h_{11/2} \otimes \nu h_{11/2}^{-1}$  as shown in Ref. [18]. Compared with the data of  $^{98}\text{Tc}$ , it is found that the results with  $\gamma = 38^{\circ}$  can give the best agreement. Both the trend

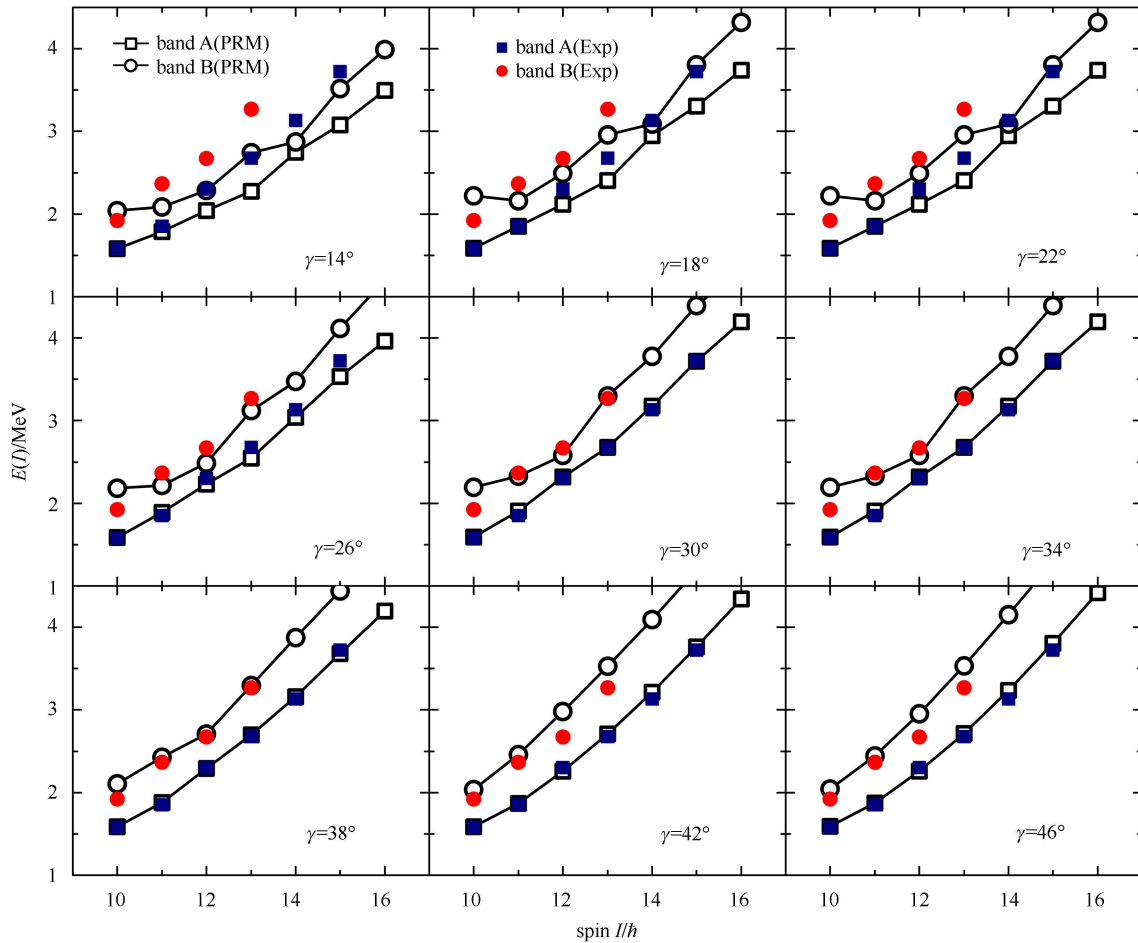


Fig. 1. The energy spectra of the two lowest bands A and B in  $^{98}\text{Tc}$  calculated by PRM with the configuration  $\pi g_{9/2} \otimes \nu h_{11/2}$  for different triaxiality parameter  $\gamma$ , in comparison with the corresponding data available [9].

of the energy as the spin and the amplitude of the energy separation between two bands are excellently reproduced.

### 3.3 $B(M1)/B(E2)$ ratios

The calculated intraband  $B(M1)/B(E2)$  ratios for the doublet bands in  $^{98}\text{Tc}$  are presented in Fig. 2, together with the available data. For  $\gamma \leq 22^\circ$ , an odd-even spin staggering of the calculated  $B(M1)/B(E2)$  ratios is very obvious, and decreases gradually as the  $\gamma$  values increase. However, this staggering is very irregular, namely the phase is not the same for the doublet bands. The  $B(M1)/B(E2)$  ratios for band A are big at odd spins and small at even spins, while the values for band B are big for spin 11, 14, 16 and small for spin 12, 13, 15. It should be mentioned that such irregular results may be very instructive, because that the observed doublet bands in  $^{106}\text{Ag}$  [6] show exactly the same irregular  $B(M1)/B(E2)$  staggering phase, which has been difficult to understand. Compared with the  $B(M1)/B(E2)$  data in  $^{98}\text{Tc}$ , it

can be seen that good agreement could also be given by the  $\gamma = 38^\circ$  case, where the best energy description is given.

### 3.4 E2 and M1 transitions

As the PRM results with  $\gamma = 38^\circ$  give a good description for the observed data, we further show the absolute  $B(M1; I \rightarrow I-1)$  and  $B(E2; I \rightarrow I-2)$  transition probabilities of the PRM calculated results with  $\gamma = 38^\circ$  in Fig. 3, which is used as a prediction for future experiments on lifetime measurement. For  $B(E2)$ , the interband values are very small and the intraband ones gradually increase as the spin increases. For  $B(M1)$ , the interband values are small and the intraband ones gradually increase as the spin increases. In addition, both the intraband  $B(E2)$  and  $B(M1)$  of Band B are larger than those of Band A. This character is very different from the ideal chiral picture, where the properties of the doublet bands should be very similar [19].

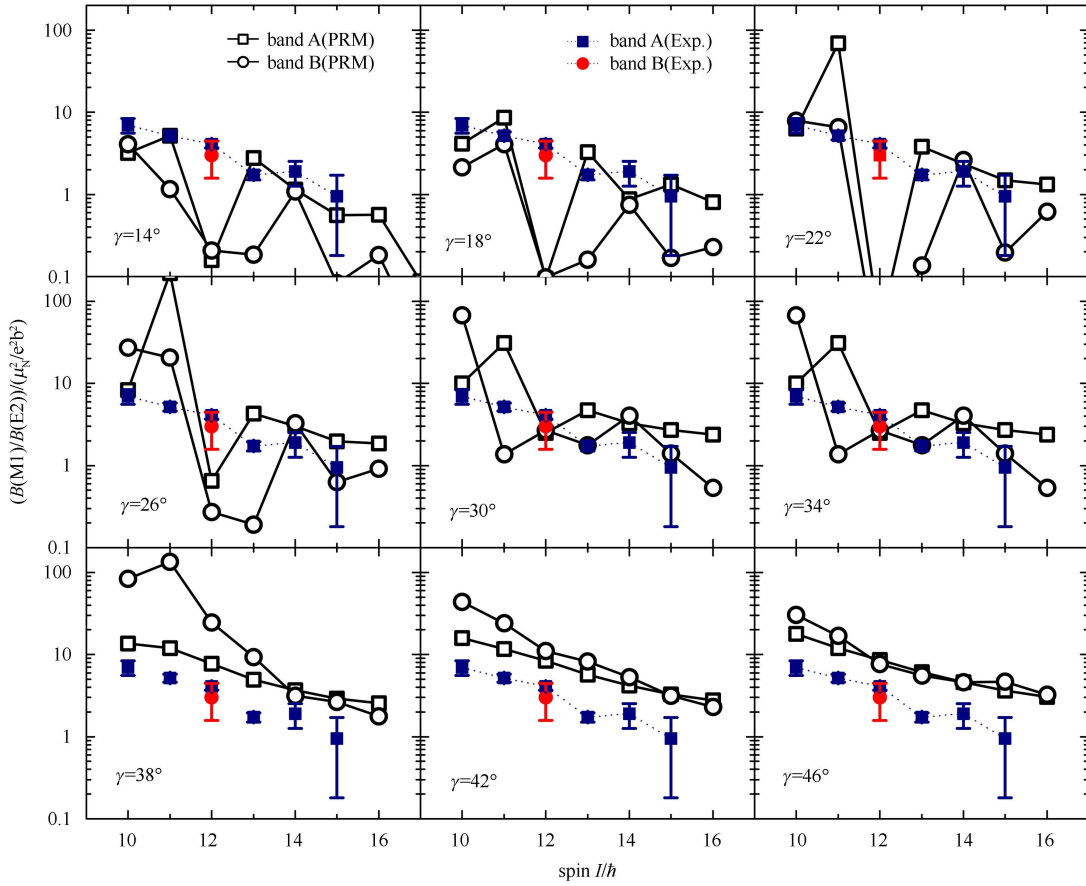


Fig. 2. The intraband  $B(M1)/B(E2)$  ratios for the doublet bands in  $^{98}\text{Tc}$  calculated by PRM, in comparison with the corresponding data available [9].

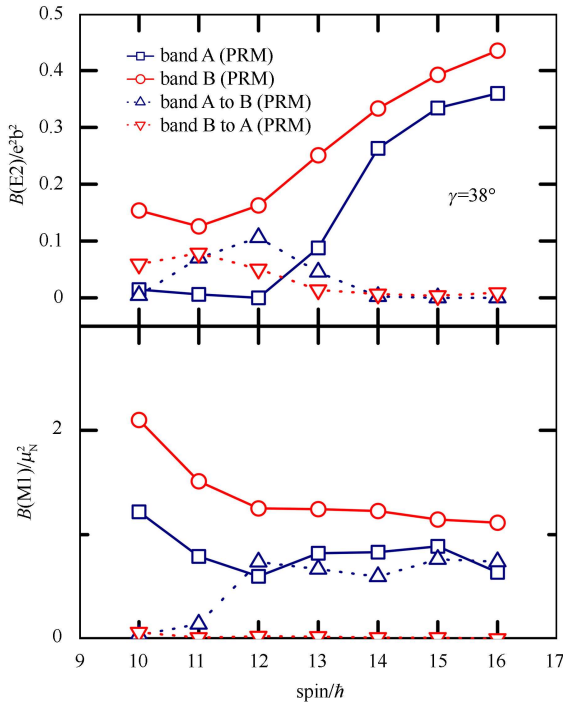


Fig. 3. The intraband and interband  $B(M1)$  and  $B(E2)$  values calculated by means of PRM with  $\gamma = 38^\circ$  for the doublet bands in  $^{98}\text{Tc}$ .

### 3.5 Chiral geometry

In order to investigate the chiral geometry, the root mean square values of the angular momentum components for the core  $R_k = \sqrt{\langle \hat{R}_k^2 \rangle}$ , the valence neutron  $J_{nk} = \sqrt{\langle \hat{J}_{nk}^2 \rangle}$  and the valence proton  $J_{pk} = \sqrt{\langle \hat{J}_{pk}^2 \rangle}$  for the bands A and B are calculated similarly as in Ref. [11] and presented in Fig. 4, in which  $k=i, s, l$  respectively represent the intermediate, short and long axis. As shown in Fig. 4, the core angular momentum mainly aligns along the  $i$ -axis and  $l$ -axis, while the angular momentum of the  $h_{11/2}$  valence neutron mainly aligns along the  $s$ -axis. The  $g_{9/2}$  quasiproton aligns along the  $i$ -axis for band A, while it has angular momentum components along all the three axis for band B. As the total angular momentum increases, the collective angular momentum increases gradually. The three angular momenta together form the nonplanar rotation. However, the valence proton gives the relatively small contribution for such nonplanar total angular momenta, which is very different from the ideal chiral picture.

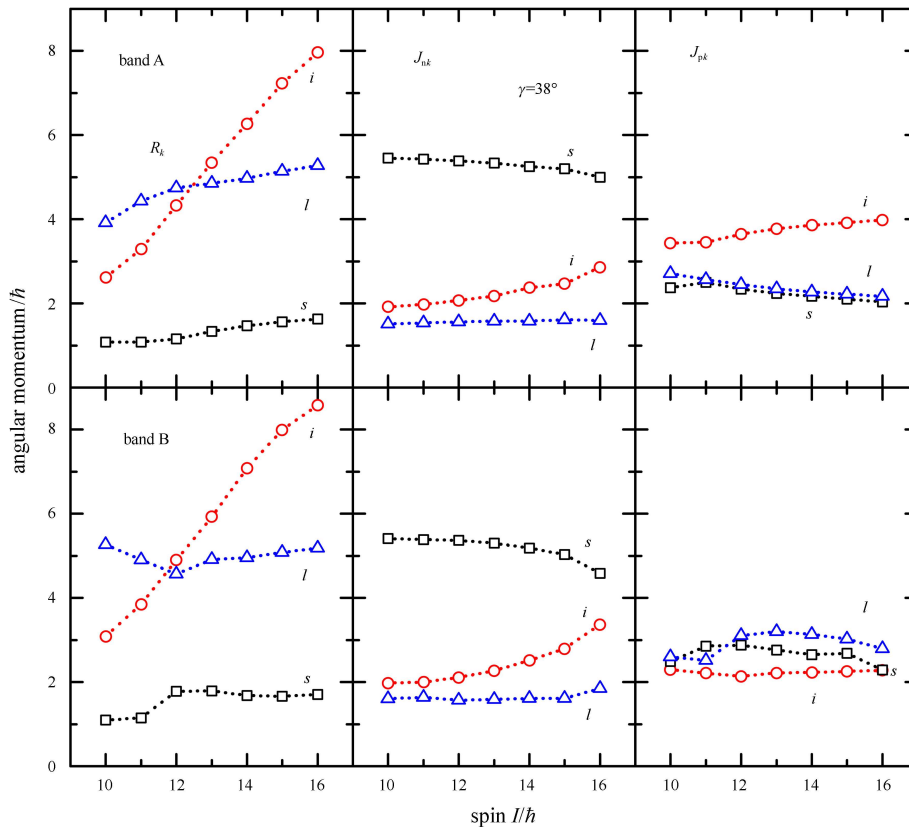


Fig. 4. The root mean square values of the angular momentum components for the core  $R_k$ , the valence neutron  $J_{nk}$  and the valence proton  $J_{pk}$  calculated by PRM with  $\gamma = 38^\circ$  for the doublet band in  $^{98}\text{Tc}$ , in which  $k=i, s, l$  respectively represent the intermediate, short and long axis.

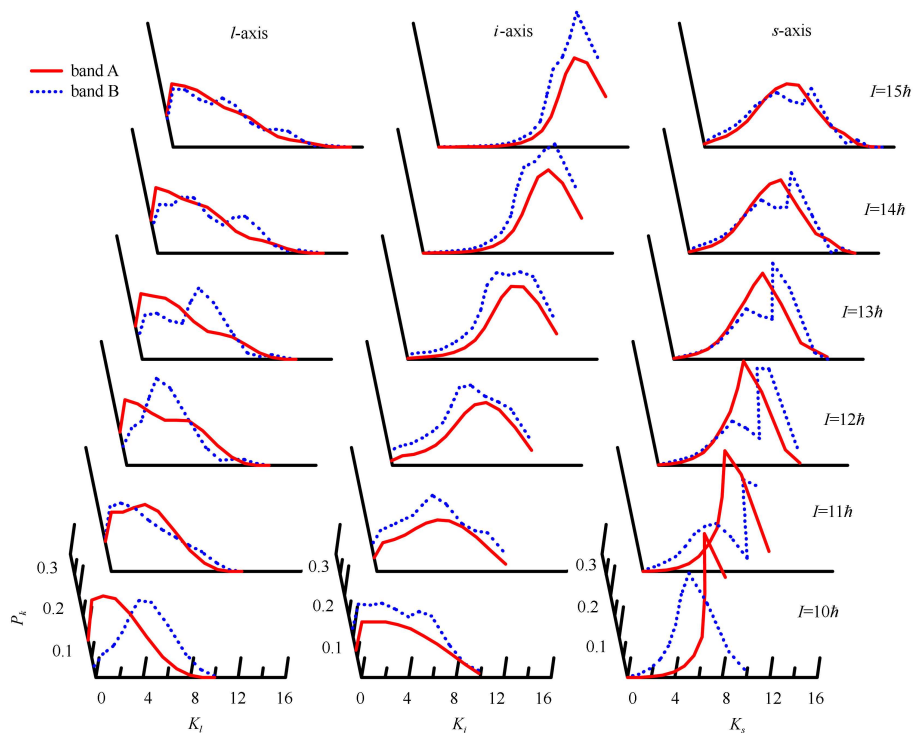


Fig. 5. The probability distributions for projection of the total angular momentum on the long ( $l$ -), intermediate ( $i$ -) and short ( $s$ -) axis in PRM with  $\gamma = 38^\circ$  for the doublet bands in  $^{98}\text{Tc}$ .

Further understanding the evolution of the chirality with angular momentum, the probability distributions for the projection of the total angular momentum [11] along the  $l$ -,  $i$ - and  $s$ -axes in PRM with  $\gamma = 38^\circ$  are given in Fig. 5 for the doublet bands in  $^{98}\text{Tc}$ . At the lower spin, the probability distribution of  $K_l$ , namely the projection of the total angular momentum along the  $l$ -axis, differs for two bands. As the spin increases, the probability distributions of  $K_l$ ,  $K_i$ ,  $K_s$  are almost the same for the two bands. They can form the nonplanar total angular momenta and chiral geometry. However, the probability distribution of  $K_l$  has its peaks near  $K_l = 0$ , namely the nonplanar total angular momenta is close to the  $i$ - $s$  plane, which is different from the ideal chiral picture.

## 4 Conclusion

The candidate chiral doublet bands in  $^{98}\text{Tc}$  are theoretically studied for the first time via the triaxial particle rotor model. The configuration  $\pi g_{9/2} \otimes \nu h_{11/2}$  is adopted in the calculation, with the proton Fermi levels supposed to be near the middle of the  $\pi g_{9/2}$  sub-

shell. The influence of the triaxial deformation  $\gamma$  on the properties of the doublet bands is presented. It is found that the observed energies and  $B(M1)/B(E2)$  ratios in the doublet bands in  $^{98}\text{Tc}$  can be well described by the PRM calculation with  $\gamma = 38^\circ$ . The absolute  $B(M1)$  and  $B(E2)$  transition probabilities have been presented, which should encourage future experiments on lifetime measurement.

Based on the analysis of angular momentum components and the probability distributions for the projection of the total angular momentum, the chiral geometry in  $^{98}\text{Tc}$  is discussed. The nonplanar total angular momenta can be formed, however the nonplanar total angular momenta are close to the  $i$ - $s$  plane. Such chiral geometry in  $^{98}\text{Tc}$  is very different from the ideal chiral picture.

The discussions presented here would be helpful to further understand those candidate chiral nuclei, in which the chirality deviates from the ideal chiral picture.

*We wish to thank Prof. ZHU Sheng-Jiang from Tsinghua University for his helpful discussions.*

## References

- 1 Frauendorf S, MENG J. Nucl. Phys. A, 1997, **617**: 131
- 2 MENG J, ZHANG S Q, J. Phys. G, 2010, **37**: 064025
- 3 Vaman C, Fossan D B, Koike T et al. Phys. Rev. Lett., 2004, **92**: 032501
- 4 Joshi P, Jenkins D G, Raddon P M et al. Phys. Lett. B, 2004, **595**: 135
- 5 Timár J, Vaman C, Starost K et al. Phys. Rev. C, 2006, **73**: 011301(R)
- 6 Joshi P, Carpenter M P, Fossan D B et al. Phys. Rev. Lett., 2007, **98**: 102501
- 7 Timár J, Koike T, Pietralla N et al. Phys. Rev. C, 2007, **76**: 024307
- 8 Joshi P, Wilkinson A R, Koike T et al. Eur. Phys. J. A, 2005, **24**: 23
- 9 DING H B, ZHU S J, WANG J G et al. Chin. Phys. Lett., 2010, **27**: 072501
- 10 ZHANG S Q, QI B, WANG S Y, MENG J. Phys. Rev. C, 2007, **75**: 044307
- 11 QI B, ZHANG S Q, MENG J et al. Phys. Lett. B, 2009, **675**: 175
- 12 Mukhopadhyay S, Almeheed D, Garg U et al. Phys. Rev. Lett., 2007, **90**: 172501
- 13 WANG S Y, ZHANG S Q, QI B et al. Phys. Rev. C, 2008, **77**: 034314
- 14 WANG S Y, ZHANG S Q, QI B et al. Chin. Phys. C, 2009, **33(S1)**: 37–39
- 15 QI B, ZHANG S Q, WANG S Y et al. Phys. Rev. C, 2011, **83**: 034303
- 16 QI B, WANG S Y, LIU C et al. Nuclear Structure in China 2010. Proceedings of the 13th National Conference on Nuclear Structure in China (NSC2010). World Scientific: Singapore, 2011. 165–168
- 17 Koike T, Starosta K, Hamamoto I. Phys. Rev. Lett., 2004, **93**: 172502
- 18 QI B, ZHANG S Q, WANG S Y et al. Phys. Rev. C, 2009, **79**: 041302(R)
- 19 Petrache C M, Hagemann G B, Hamamoto I, Starosta K. Phys. Rev. Lett., 2006, **96**: 112502